# Study of Light Emission Enhancement in Nanostructured InGaN/GaN Quantum Wells

Cheng-Yu Chang, *Student Member, IEEE*, and Yuh-Renn Wu, *Member, IEEE*

***Abstract*—Recently, InGaN/GaN quantum wells with different nanostructures such as nanoholes and nanorods have been proposed to enhance the light emitting efficiency. This paper calculates the influence of nanostructures to the strain and band profile of the quantum well. The effects of strain relaxation and surface states are analyzed, which could possibly influence the diode emission properties. Our calculation results show that the strain relaxation and the surface state pinning play important roles in enhancing the light emission, reducing the quantum confined Stark effect, and causing the blue shift of the spectrum. Our calculation results provide useful information in analyzing emission properties of nanohole arrays and similar structures.**

***Index Terms*—GaN, InGaN, nanohole, strain relaxation, valence force field model, surface state, quantum well.**

## I. Introduction

In recent years, III-nitride wide bandgap semiconductors have been widely used in optoelectronic devices, such as blue and green light-emitting diodes (LEDs) [1], [2]. However, it is difficult to obtain a high efficiency quantum well LED due to the strong strain induced in the quantum well because of the large lattice-mismatch between InN and GaN crystals. The strong strain leads to a strong piezoelectric polarization in the quantum well [3] and results in the quantum confined-Stark effect (QCSE). The QCSE reduces the carrier recombination rates and limits the device performance. Recently, devices with nanostructures such as nanorods [4], nanocolumns, nanohole arrays, and photonic crystal structure LEDs [5], [6] have shown improvement in device performance. These structures are either designed to have a stronger confining cavity of laser applications or are designed to enhance the light extraction efficiency [7], with the possibility of strain relaxation in the quantum well [8], [9].

In this paper, we use $In_{0.3}Ga_{0.7}N$/GaN green LEDs with nanohole structures to study the enhancement of IQE and analyze the emission property. As we know, when these nanostructures are fabricated in LED devices, not only are the light propagation properties changed but also the electronic band structures. Hence, it is important to know how these nanostructures couple into the quantum well, influence the band structure, and change the light emission properties. Recently, reports [10]–[16] on nanocolumns or nanoporous structures have shown a stronger emission, a shorter radiative lifetime, a smaller QCSE effect, and a blue shift of the emission peak compared to normal structures. The stronger emission rate may be partially due to the improvement of the light extraction efficiency. However, it is difficult to explain the shorter radiative lifetime and blue shift of the spectrum. In this work, we have made a complete calculation to understand the roles of strain, surface states [17], [18], and the barrier thickness [19], [20] in changing the band structure of these nanohole structures. Nanohole structures with different GaN cap thickness are studied. The three-dimensional (3-D) valence force field model (VFF) [21] for strain calculation and Poisson and Schrödinger and drift-diffusion solver for band structure calculation are applied in this study. In the following sections, we will address the simulation models we applied and show how the nanohole structure affects the band profile and enhances the radiative recombination rates.

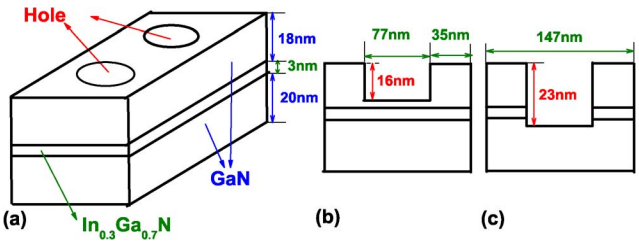


Fig. 1. A schematic of the nanohole structure. The hole depths are 16 nm and 23 nm.

## II. Theoretical Model

The device structures are shown in Fig. 1. Holes with different depths are in the center of the device with a diameter of ~77 nm. The periodic boundary condition is used in the lateral direction for strain calculation for a nanohole array. The spacing between holes is around 147 nm. The $In_{0.3}Ga_{0.7}N$ quantum well thickness is around 3 nm. The top GaN cap layer thickness is 18 nm. From our studies, a GaN cap layer of thickness $>20$ nm has similar results as the 18 nm for the GaN cap LED structure.

To analyze these structures as shown in Fig. 1(b) and (c), we use the following processes: 1) apply the 3-D VFF model [21] to calculate the strain distribution of the nanohole array structures; 2) calculate the piezoelectric polarization charges with the obtained strain distribution; 3) use the self-consistent Poisson,

Manuscript received September 24, 2009; revised December 02, 2009 and December 19, 2009. Current version published March 10, 2010. This project was supported in part by the Ministry of Education, Taiwan, under project "Aim for Top University", and in part by the National Science Council, Taiwan, under Grant NSC-97-2221-E002-050 and Grant NSC-98-2221-E002-037-MY2.

The authors are with the Graduate Institute of Photonics and Optoelectronics and Department of Electrical Engineering, National Taiwan University, Taipei 10617, Taiwan (e-mail: yrwu@cc.ee.ntu.edu.tw).

Color versions of one or more of the figures in this paper are available online at http://ieeexplore.ieee.org.

Digital Object Identifier 10.1109/JQE.2010.2040515

Schrödinger and drift-diffusion solver developed in our laboratory [22] to solve the band structures; and 4) calculate spontaneous emission rate and emission spectrum.

In the first step, we calculate the strain in the nanohole array with the VFF model. The VFF model is a microscopic model, where the interactions between each atom and its nearby atoms are considered. The total elastic energy is expressed as a function of atomic positions, $\vec{R}_i$, using the summation of bond stretching $(V_2)$ and bond bending $(V_3)$ terms:

$$\begin{aligned} E_{AE} &= \sum_{ij} V_2(\vec{R}_i - \vec{R}_j) + \sum_{ijk} V_3(\hat{\theta}_{ijk}) \\ &= \frac{1}{2}\sum_i \sum_j^{nn} \frac{3\alpha_{ijk}}{8\left(d_{ij}^0\right)^2}\left[(\vec{R}_i - \vec{R}_j)^2 - \left(d_{ij}^0\right)^2\right]^2 \\ &\quad + \frac{1}{2}\sum_i \sum_{j,k>j}^{nn} \frac{3\beta_{ijk}}{8d_{ij}^0 d_{ij}^0}\left[(\vec{R}_j - \vec{R}_i)\cdot(\vec{R}_k - \vec{R}_i)\right. \\ &\quad \left. - \cos\theta_0 d_{ij}^0 d_{ij}^0\right]^2 \end{aligned} \tag{1}$$

where $d_{ij}^0$ denotes the unstrained bond length between atoms i and j, and $\theta_0$ is the unstrained bond angle, and $\cos\theta_0 = -1/3$. The bond stretching $\alpha$ and bond bending $\beta$ force constants are listed in Mattila *et al.* [21]. We have applied these models for studying the strain distribution in quantum dot [23] and nanorod systems [9], [24]. With this model, we can obtain the strain distribution in the nanohole structure. The piezoelectric polarization can be calculated by

$$P_{pz} = e_{31}(\epsilon_{xx} + \epsilon_{yy}) + e_{33}\epsilon_{zz} \tag{2}$$

where the $\epsilon_{xx}$, $\epsilon_{yy}$, and $\epsilon_{zz}$ are the strain distribution in the device. $e_{31}$ and $e_{33}$ are piezoelectric coefficients [3]. With the calculated polarization distribution, the induced piezoelectric polarization charge $\rho_{pz}(z)$ can be calculated by

$$\rho_{pz}(z) = \frac{(P_{ez}(z+dz) + P_{\rm sp}(z+dz) - P_{ez}(z) - P_{\rm sp}(z))}{dz} \tag{3}$$

where $P_{\rm sp}$ is the spontaneous polarization of nitride alloy. Finally, we use a self-consistent Poisson, drift-diffusion, and Schrodinger equation solver [22] to obtain the band profile, eigen levels, and wave functions of the quantum well structure. The Poisson equation, drift-diffusion equation, and continuity equation can be written as

$$\nabla^2 V = \frac{n - p + N_A - N_D}{\epsilon} \tag{4}$$

$$J_n = -\mu_n n(z)\nabla V(z) + qD_{n,p}\nabla n(z) \tag{5}$$

$$J_p = \mu_p p(z)\nabla V(z) - qD_p \nabla p(z) \tag{6}$$

$$\nabla J_{n,p} = \pm R \mp G \tag{7}$$

where $V$ is the band potential of the device. $J_n$ and $J_p$ are the electron and hole current, respectively. $R$ is the carrier recombination term including the radiative and non-radiative recombination and $G$ is the carrier generation term which can come from the light absorption, etc.

To simulate the PL spectrum observed by the experimental results, we use the generation term in the drift-diffusion equation to model the electron and hole generation from the absorption of light. At the end, the emission rates can be calculated by

$$\begin{aligned} R_{\rm sp} &= \int d(\hbar\omega)\frac{e^2 n_r \hbar\omega}{m_0^2 \varepsilon_0 c^3 \hbar^2}\sum_{i,j}\int \frac{2}{(2\pi)^2} d^2k |\hat{a}\cdot\vec{p}_{ij}|^2 \\ &\quad \times \frac{1}{\sqrt{2\pi}\sigma}\exp\left(\frac{-(E_{i,j} - \hbar\omega)^2}{2\sigma^2}\right) f^e f^h \ (\mathrm{cm}^{-2}\mathrm{s}^{-1}) \end{aligned} \tag{8}$$

where $|\hat{a}\cdot\vec{p}_{ij}|^2$ is the momentum matrix element square between state $i$ and $j$. The effect of electron–hole overlap is included in this term. $f^e$ and $f^h$ are Fermi–Dirac distribution function. $\sigma$ is the inhomogeneous broadening factor and $E_{i,j}$s are the energy interval from state $i$ and $j$. After obtaining the total emission rate $R_{\rm sp}$, the radiative lifetime is estimated by

$$\tau_r = n_{2D}/R_{\rm sp}(s) \tag{9}$$

where $n_{2d}$ is the 2-D carrier density in the quantum well obtained from our solver. We carefully tuned the generation term, $G$, in the solver to obtain a similar $n_{2D}$ in each case for comparison.

## III. Results and Discussion

We calculated the strain distribution of the two different cases as shown in Fig. 2 in order to realize the effect of the strain relaxation mechanism in these nanohole structures. Fig. 2(a) and (b) show the strain tensors $\epsilon_{xx}$ and $\epsilon_{zz}$ of the 16 nm-hole-depth case, respectively. The hole is etched to close to the quantum well region but does not penetrate through the quantum well. Fig. 2(c) and (d) show the strain tensors $\epsilon_{xx}$ and $\epsilon_{zz}$ with the hole depth equal to 23 nm, respectively. The hole has penetrated through the quantum well. It is clear to see that for the 16 nm case, the strain relaxation effect is weak except near the corner edge of the device. The tensile strain $\epsilon_{zz}$ under the hole region is relaxed by $\sim$10% compared to the unetched region. For the 23 nm-hole-depth case, we can see a clear strain relaxation from the edge of the hole near the quantum well and the cap layer region. The maximum strain relaxation of the compressive strain, $\epsilon_{xx}$, near the hole edge is estimated to be around 80%. The strain relaxed region is around 20–30 nm from the hole edge. Our calculation shows that the strain does not release too much unless the etched hole penetrates through the quantum well. As a result, the blue shift caused by strain relaxation should not be observed in the structure with a 16 nm etching depth [14]–[16]. However, the experimental data does show a clear blue shift. Therefore, we look into other possible reasons such as the effect of surface states [17], etc.

Calculations are first performed on the band structures and emission properties of these devices in order to realize the physics inside the device. We can estimate the piezoelectric polarization, solve the band structures, and calculate the emission rate and spectrum with the calculated strain information. As mentioned earlier, the generation term in the drift-diffusion equation is used to model the electron and hole pair generation from light absorption with the generation term $G$ in (7). Simulation of the PL emission can be performed by tuning the generation term. The nanohole structure with 23 nm hole depth might have a larger blue shift due to the strain relaxation, as

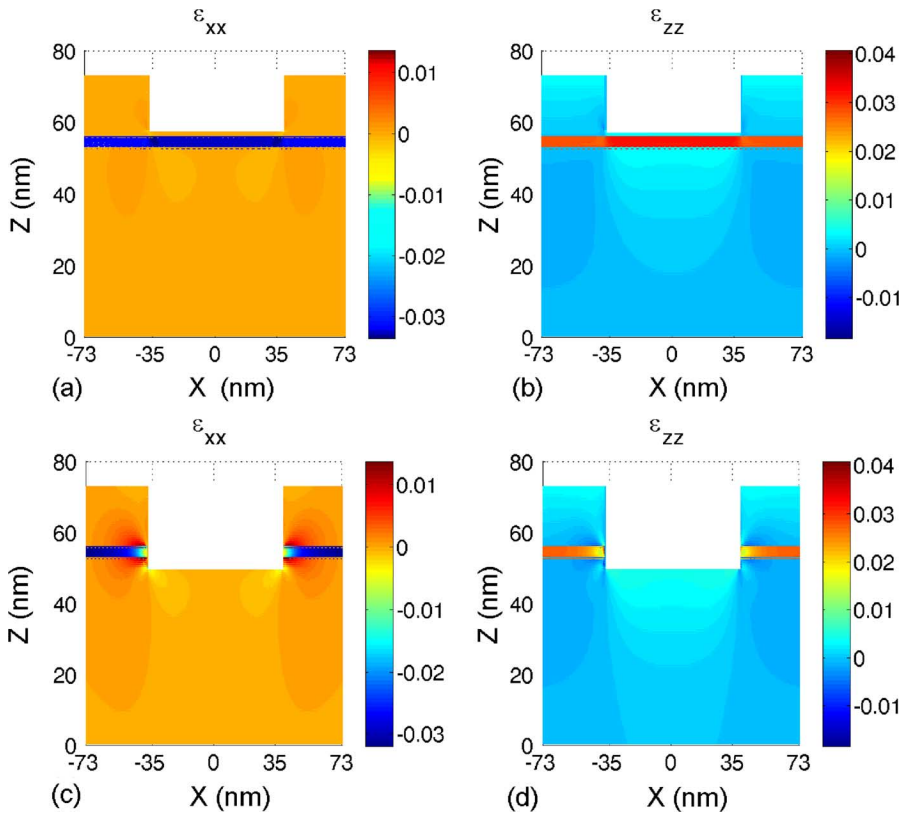


Fig. 2. The calculated strain tensor (a) $\epsilon_{xx}$ and (b) $\epsilon_{zz}$ of the nanohole structure with 16 nm hole depth. The calculated (c) $\epsilon_{xx}$ and (d) $\epsilon_{zz}$ of the nanohole structure with 23 nm-column hole depth.

shown in the strain data in Fig. 2. However, the fermi level is usually pinned at levels of the surface states (∼0.9 eV below conduction band for GaN) because of the effect of surface states at the air/GaN interface [17], [18], [25]. The effect of the surface states is negligible if the cap layer is thick enough. However, for the 16 nm-hole-depth case, the distance from the surface state to the quantum well region is only 2 nm. Therefore, the pinning position of the surface state will strongly affect the band bending in the GaN cap layer and in the InGaN quantum well. Fig. 3 shows the calculated band structures of the 16 nm nanohole structure at the center of the hole and at the unetched region. The carrier density $n_{2d}$ is tuned to $\sim 1.0 \times 10^{13}$ cm$^{-2}$ in the quantum well region. We can see that the thicker GaN cap layer leads to a stronger band bending due to the strong piezoelectric polarization field. When the top GaN cap layer is too thin as shown in Fig. 3(a), the band bending at the GaN layer is not large enough. Therefore, the potential on the left side of the InGaN quantum well is lifted up, which reduces the QCSE significantly.

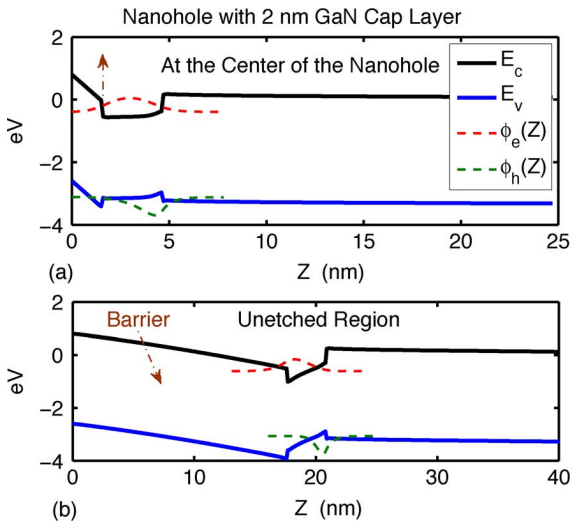


Fig. 3. The band structures and wavefunction of 16 nm nanohole structure at (a) X = 0.0 nm (etched region) and (b) X = 64 nm (unetched region).

Fig. 4(b) shows the calculated emission spectrum at a different position for the 16 nm depth nanohole. The positions at $X = 40.6$ nm and $X = 63$ nm are at the unetched area (pink dash dotted line and blue dotted line). Although there is a slight strain relaxation at $X = 40.6$ nm compared to the position at $X = 63$ nm, this effect is weak and does not make a difference as shown in Fig. 4(b). The positions at $X = 37.4$ nm and $X = 0.0$ nm (red line and green dashed line) are inside the hole area. Also, the strain relaxation does not play an important role if we compare these two positions. However, as mentioned earlier, the band bending is small so that the QCSE effect is much weaker due to the surface states pinning effect. The oscillator strength is mainly decided by the square of the electron–hole overlap for InGaN quantum well LEDs. The smaller QCSE leads to stronger radiative recombination rates. Our results show that the emission rate is enhanced by 13 times compared to the unetched region. Our calculation result also shows

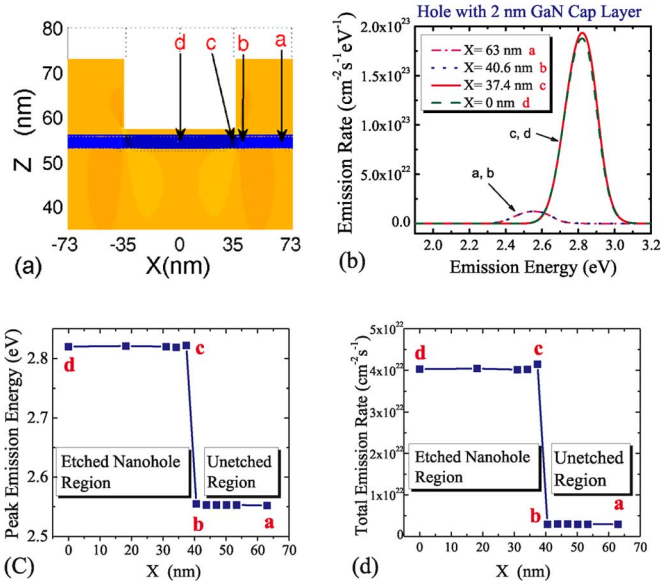


Fig. 4. (a) The strain distribution and the definition of a, b, c, and d points. (b) The calculated emission spectrum at a, b, c, and d points in 16 nm nanohole structure. Note that the curves for points a and b are almost overlapped and the curves for point c and d are also mostly overlapped. (c) The emission peak energy and (d) the total emission rate versus different positions for the 16 nm nanohole structure.

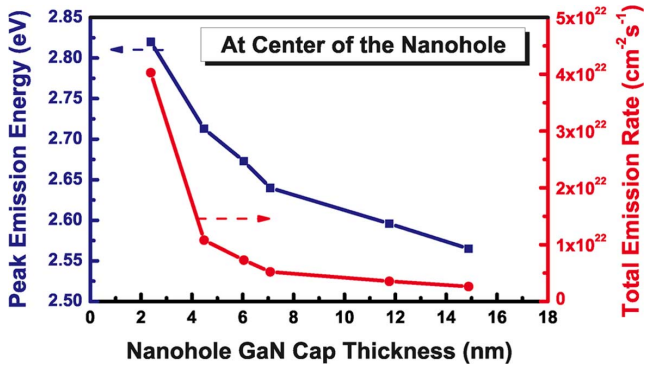


Fig. 5. The calculated emission strength and emission peak energy versus different nanohole GaN cap layer thickness (nanohole distance to the quantum well).

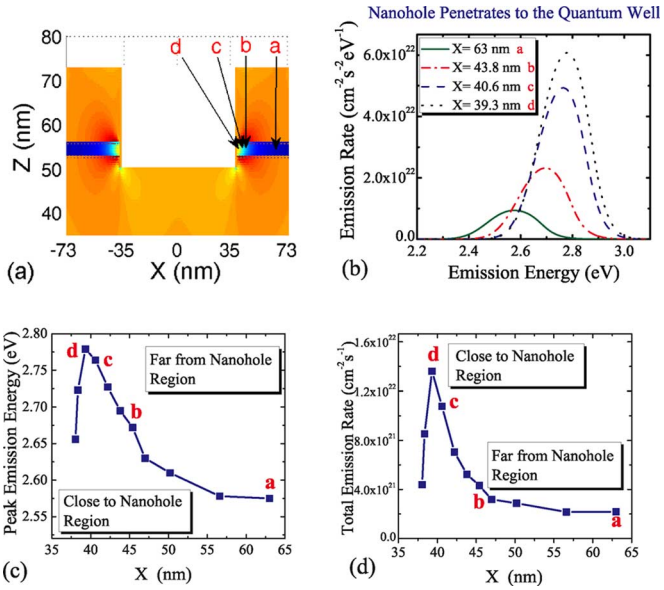


Fig. 6. (a) The strain distribution and the definition of a, b, c, and d points. (b) The calculated emission spectrum at a, b, c, and d points for the 23 nm nanohole structure. (c) The emission peak energy and (d) the total emission rate versus different positions for the 23 nm nanohole structure.

a blue shift of a maximum of 270 meV for the 16 nm-hole-depth case compared to the unetched region. The estimated radiative lifetimes at the carrier injection density close to $\sim 1.0 \times 10^{13}$ cm$^{-2}$ ($\sim 3.3 \times 10^{19}$ cm$^{-3}$ for 3 nm quantum well) for the unetched and etched regions are around 3.3 ns and 0.3 ns, respectively. The radiative lifetime will depend on the injection carrier density and these results are for the high injection carrier density case. For the lower injection density case, the enhancement is even stronger because of the strong QCSE effect in the unetched region. Fig. 4(c) and (d) show the emission peak energy and emission rate versus different positions from the edge, respectively. As shown in Fig. 4(c) and (d), the etched and unetched areas have a significant difference in the emission properties. Note that the total emission spectrum of the entire device would depend on the ratio of the unetched area size to the etched area size.

It would be important to understand how the depth of the hole influences the emission spectrum. Therefore, we calculated the emission rates of the different nanohole depths as shown in Fig. 5. We can find that for the nanohole region where the GaN cap thickness is smaller than 7 nm, the emission rate and emission peak start to have a significant change. This implies that the surface state effects need to be considered more seriously when the GaN cap thickness is within 7 nm. The blue shift caused by surface states pinning also decreases rapidly when the nanohole surface is away from the quantum well if the etched surface is far from the active layer.

The emission property is different from the 16 nm one as the hole penetrates the quantum well for the 23 nm-nanohole-depth case as shown in Fig. 6(a). In the hole region, the quantum well is removed and there is no emission from the hole region. As shown in Fig. 6(a), there is a strong strain relaxation near the edge of the hole [b, c, and d points shown in Fig. 6(a)]. Fig. 6(b) shows the calculated emission spectrum at the points, a, b, c, and d. At the point d ($X = 39.3$ nm), the strain relaxation of the quantum well reaches the maximum and the emission rate also reaches the maximum as shown in Fig. 6(b). Fig. 6(c) and (d) show the emission peak and emission rates versus different positions $X$, respectively. We can see that the affected region is within 20 nm from the hole edge since the strain is gradually relaxed from the edge. This strain relaxation effect is also observed in the nanorod structures [9], [24]. A maximum 200 meV blue shift in the emission peak and a 0.75 ns radiative lifetime are estimated at the maximum strain relaxed region at $n_{2d}$ close to $\sim 1.0 \times 10^{13}$ cm$^{-2}$. The emission rate increases 6.3 times compared to the unrelaxed region. Note that the experimental measurement may not observe this large peak shift and the total emission spectrum should be estimated through the integration of emission spectrum at different regions. Therefore, it depends on both the hole diameter and the hole spacing. The broadening

of the emission spectrum is expected. Also, as the hole penetrates the quantum well, there might be surface states forming at the sidewall, which might make the band bending horizontal. So, it might push the carrier slightly to the center. However, the QCSE effect is along the c-axis, and therefore, this band bending will not directly influence the red or blue shift of the emission spectrum.

Our calculations show that the emission rate has a significant enhancement when the nanohole is close to the quantum well. However, we need to be careful about the carrier leakage and the surface state trapping. To avoid the influence of the surface state trapping, a GaN cap layer thickness larger than 4 nm is suggested to avoid the electron wavefunction extending to the surface.

It is difficult to have a quantitative comparison from the published experimental work. From the published work [10]–[16], the possible influences of surface states are not taken care of and the detail about the actual etching depth is not determined carefully. Therefore, it is difficult to determine the real depth of the hole to quantitatively understand the possible influences of the surface state or the strain relaxation. We hope our studies can provide sufficient information to explain experimental results.

## IV. Conclusion

In conclusion, we have analyzed the emission characteristic of InGaN/GaN LEDs with different nanohole depth. The emission property of the nanohole increases significantly when the hole is close to or penetrates the quantum well. One may be due to the effect of surface states and the other one might be due to the strain relaxation. Both effects lead to the blue shift of the spectrum and the increase of radiative recombination rates. To avoid surface state trapping, the GaN cap layer thickness is suggested to be around 4 nm to have the best performance. Our calculations on the strain relaxation and surface states pinning provide useful information for analyzing the spectrum shift in the nanohole array and are very important factors to be considered when making similar structures, such as photonic crystal structures, nanocolumns, and nanorods.

## References


[1] S. Nakamura, M. Senoh, N. Iwasa, S. Nagahama, T. Yamada, and T. Mukai, "Superbright green InGaN single-quantum-well-structure light-emitting-diodes," *Jpn. J. Appl. Phys. Part 2—Lett.*, vol. 34, no. 10B, pp. L1332–L1335, 1995.

[2] Y. Narukawa, J. Narita, T. Sakamoto, K. Deguchi, T. Yamada, and T. Mukai, "Ultra-high efficiency white light emitting diodes," *Jpn. J. Appl. Phys. Part 2—Lett. & Express Lett.*, vol. 45, no. 37–41, pp. L1084–L1086, 2006.

[3] O. Ambacher, J. Majewski, C. Miskys, A. Link, M. Hermann, M. Eickhoff, M. Stutzmann, F. Bernardini, V. Fiorentini, V. Tilak, B. Schaff, and L. F. Eastman, "Pyroelectric properties of Al(In)GaN/GaN hetero- and quantum well structures," *J. Phys.—Condensed Matter*, vol. 14, no. 13, pp. 3399–3434, 2002, PII S0953-8984(02)29 173-0.

[4] W. Q. Han and A. Zettl, "Pyrolysis approach to the synthesis of gallium nitride nanorods," *Appl. Phys. Lett.*, vol. 80, no. 2, pp. 303–305, 2002.

[5] H. Matsubara, S. Yoshimoto, H. Saito, J. L. Yue, Y. Tanaka, and S. Noda, "GaN photonic-crystal surface-emitting laser at blue-violet wavelengths," *Science*, vol. 319, no. 5862, pp. 445–447, 2008.

[6] K. McGroddy, A. David, E. Matioli, M. Iza, S. Nakamura, S. DenBaars, J. S. Speck, C. Weisbuch, and E. L. Hu, "Directional emission control and increased light extraction in GaN photonic crystal light emitting diodes," *Appl. Phys. Lett.*, vol. 93, no. 10, p. 103502, 2008.

[7] T. S. Kim, S. M. Kim, Y. H. Jang, and G. Y. Jung, "Increase of light extraction from GaN based light emitting diodes incorporating patterned structure by colloidal lithography," *Appl. Phys. Lett.*, vol. 91, p. 171114, 2007.

[8] C. H. Chiu, M. H. Lo, C. F. Lai, T. C. Lu, H. W. Huang, Y. A. Chang, T. H. Hsueh, C. C. Yu, H. C. Kuo, S. C. Wang, C. F. Lin, and Y. K. Kuo, "Optical properties of $In_{0.3}Ga_{0.7}N$/GaN green emission nanorods fabricated by plasma etching," *Nanotechnology*, vol. 18, no. 33, p. 335706, 2007.

[9] P. C. Yu, C. H. Chiu, Y. R. Wu, H. H. Yen, J. R. Chen, C. C. Kao, H. W. Yang, H. C. Kuo, T. C. Lu, W. Y. Yeh, and S. C. Wang, "Strain relaxation induced microphotoluminescence characteristics of a single InGaN-based nanopillar fabricated by focused ion beam milling," *Appl. Phys. Lett.*, vol. 93, no. 8, p. 081110, 2008.

[10] Y. Kawakami, S. Suzuki, A. Kaneta, M. Funato, A. Kikuchi, and K. Kishino, "Origin of high oscillator strength in green-emitting InGaN/GaN nanocolumns," *Appl. Phys. Lett.*, vol. 89, no. 16, p. 163124, 2006.

[11] C. F. Lin, J. H. Zheng, Z. J. Yang, J. J. Dai, D. Y. Lin, C. Y. Chang, Z. X. Lai, and C. S. Hong, "High-efficiency InGaN-based light-emitting diodes with nanoporous GaN:Mg structure," *Appl. Phys. Lett.*, vol. 88, no. 8, p. 083121, 2006.

[12] K. Kim, J. Choi, T. S. Bae, M. Jung, and D. H. Woo, "Enhanced light extraction from nanoporous surfaces of InGaN/GaN-based light emitting diodes," *Jpn. J. Appl. Phys. Part 1—Reg. Papers, Brief Commun., Rev. Papers*, vol. 46, pp. 6682–6684, 2007.

[13] Y. D. Wang, K. Y. Zang, and S. J. Chua, "Nonlithographic nanopatterning through anodic aluminum oxide template and selective growth of highly ordered GaN nanostructures," *J. Appl. Phys.*, vol. 100, no. 5, p. 054306, 2006.

[14] C. B. Soh, S. Y. Chow, L. Y. Tan, H. Hartono, W. Liu, and S. J. Chua, "Enhanced luminescence efficiency due to carrier localization in InGaN/GaN heterostructures grown on nanoporous GaN templates," *Appl. Phys. Lett.*, vol. 93, no. 17, p. 173107, 2008.

[15] K. Y. Zang, S. J. Chua, J. H. Teng, N. S. S. Ang, A. M. Yong, and S. Y. Chow, "Nanoepitaxy to improve the efficiency of InGaN light-emitting diodes," *Appl. Phys. Lett.*, vol. 92, no. 24, p. 243126, 2008.

[16] C. C. Yang, C. F. Lin, C. M. Lin, C. C. Chang, K. T. Chen, J. F. Chien, and C. Y. Chang, "Improving light output power of InGaN-based light emitting diodes with pattern-nanoporous p-type GaN:Mg surfaces," *Appl. Phys. Lett.*, vol. 93, no. 20, p. 203103, 2008.

[17] L. H. Peng, C. M. Lai, C. W. Shih, C. C. Chuo, and J. I. Chyi, "Boundary effects on the optical properties of InGaN multiple quantum wells," *IEEE J. Sel. Topics Quantum Electron.*, vol. 9, no. 3, pp. 708–715, May 2003.

[18] G. Koley and M. G. Spencer, "Surface potential measurements on GaN and AlGaN/GaN heterostructures by scanning Kelvin probe microscopy," *J. Appl. Phys.*, vol. 90, no. 1, pp. 337–344, 2001.

[19] D. J. Kim, Y. T. Moon, K. M. Song, and S. J. Park, "Effect of barrier thickness on the interface and optical properties of InGaN/GaN multiple quantum wells," *Jpn. J. Appl. Phys. Part 1—Reg. Papers, Short Notes, Rev. Papers*, vol. 40, no. 5A, pp. 3085–3088, 2001.

[20] D. I. Florescu, J. C. Ramer, D. S. Lee, and E. A. Armour, "InGaN/GaN single-quantum-well light-emitting diodes optical output efficiency dependence on the properties of the barrier layer separating the active and p-layer regions," *Appl. Phys. Lett.*, vol. 84, no. 25, pp. 5252–5254, 2004.

[21] T. Mattila and A. Zunger, "Predicted bond length variation in wurtzite and zinc-blende InGaN and AlGaN alloys," *J. Appl. Phys.*, vol. 85, no. 1, pp. 160–167, 1999.

[22] Y. R. Wu, M. Singh, and J. Singh, "Gate leakage suppression and contact engineering in nitride heterostructures," *J. Appl. Phys.*, vol. 94, no. 9, pp. 5826–5831, 2003.

[23] Y. R. Wu, Y. Y. Lin, H. H. Huang, and J. Singh, "Electronic and optical properties of InGaN quantum dot based light emitters for solid state lighting," *J. Appl. Phys.*, vol. 105, no. 1, p. 013117, 2009.

[24] Y. R. Wu, C. Chiu, C. Y. Chang, P. Yu, and H.-C. Kuo, "Size-dependent strain relaxation and optical characteristics of InGaN/GaN nanorod LEDs," *IEEE J. Sel. Topics Quantum Electron.*, vol. 15, pp. 1226–1233, 2009.

[25] B. Jogai, "Influence of surface states on the two-dimensional electron gas in AlGaN/GaN heterojunction field-effect transistors," *J. Appl. Phys.*, vol. 93, no. 3, pp. 1631–1635, 2003.

**Cheng-Yu Chang** (S'07) received the B.S. degree in mechanical engineering in National Central University, Taiwan, in 2007, and the M.S. degree from the Graduate Institute of Photonics and Optoelectronics and Department of Electrical Engineering, National Taiwan University, Taiwan, in 2009.

His current research is focused on the device simulation on LEDs.

**Yuh-Renn Wu** (S'02–M'07) received the B.S. degree in physics and the M.S. degree in electrical engineering from National Taiwan University, Taiwan, in 1998 and 2000, respectively, and the Ph.D. degree in electrical engineering from the Department of Electrical Engineering and Computer Science at University of Michigan, Ann Arbor, in 2006.

He is currently an Assistant Professor in the Institute of Photonics and Optoelectronic and Department of Electrical Engineering, National Taiwan University. His area of research is in physics, design of optoelectronic devices and high power electronics. His current research includes the studies of nitride based quantum well, quantum wire, and quantum dot LEDs, high power and high speed electronics, ferroelectrics, and optoelectronic devices.